2017 IEEE International Conference on Cyborg and Bionic Systems
October 17 - 19, 2017, Beijing, China

Path Planning and Design for AFM based Nano-manipulation using Probability Distribution

Shuai Yuan, *Member, IEEE*, Lianqing Liu, *Member, IEEE*, Zhidong Wang, *Member, IEEE*, Jingyi Xing, Ning Xi, *Fellow*, *IEEE*, Yuechao Wang, *Member, IEEE*.

***Abstract*—In AFM nanomanipulation, the uncertainty of tip position in the task space can lead to inefficient nanomanipulation. To resolve this problem, the paper proposes a method which uses the local scan to obtain the observation distance. Then the landmark adjacency matrix is established for designing the observed landmarks. Next，colony optimization and Dijkstra's Algorithm are used to plan the tip trajectory, which reduces the cost greatly. Finally, the experiment results illustrate that the proposed algorithm can perform effective nano-manipulation.**

Keywords—AFM, Trajectory planning, Nanomanipulation, ant colony optimization, Dijkstra's Algorithm

1. Introduction

With the rapid development of nanotechnology, the semiconductor industry, such as large-scale integrated circuit manufacturing, a variety of military or civilian micro-sensors, micro structural design, have changed from the microscale into the nanoscale [1]. The technology of scanning probe microscopy is developed- to meet this requirement [2]. This kind of processing technology improves the surface morphology of the sample by the micro-tip interacting with the sample at nanometer scalesuch as mechanical force, heat, electric field, chemical reaction, so as to realize micro-nano scale processing. Because AFM has the advantages of high imaging resolution, good repeatability and strong controllability, it has become the preference for nano- manipulation and has been widely used in micro-nano device assembly. However, there are still many aspects need to be improved, for example, PZT nonlinearity and system thermal drift still exist, which leads to the uncertainty of the tip in the task space.

This research work is partially supported by the National Natural Youth Science Foundation of China (Project Codes: 61305125), Shenyang Jianzhu University Discipline Content Education Project (Project Codes: XKHY2-66), the Natural Science Foundation of University (Project Codes: 2014068) and National Post Doctor Foundation (Project Codes: 2013M530955, 2014T70265)

Shuai Yuan, Lianqing Liu, Zhidong Wang, Ning Xi, Yuechao Wang are with the State Key Lab. Robot., SIA., Chinese Academy of Sciences, Shenyang 110016, China.

Shuai Yuan, Jingyi Xing are with Shenyang Jianzhu University, Shenyang,110168, China.

Zhidong Wang is with the Dept. of Advanced Robotics, Chiba Institute of Technology, Chiba 275-0016, Japan.

Ning Xi is with the Dept. of Mechanical and Biomedical Engineering, City University of Hong Kong, Hong Kong, China.

As a result, the low efficiency of nano-manipulation hinders the development of AFM robotic nano-manipulation in Micro/Nano Device Assembly.

In AFM robotic nano-manipulation, the AFM tip acts as an end effector for constructing Micro/Nano Devices, such as assembling nanotubes onto electrodes. Figure 1 (a) shows a nano-assembly task example. Due to the non-linearity of the tip driver PZT and the temperature drift of the system, it is difficult to guarantee the accuracy of the tip position in the task space during the manipulation. Assuming that the initial position of the tip in Fig.1 (marked by the blue part of the initial position in Figure 1(b)), we move the tip to the nanotube vicinity and then push the nanotube onto the two electrodes. During the manipulation, the tip interacts with the manipulated object via point contacting. The uncertainty of the tip position leads to an uncontrollable result for manipulating the nanotube, which lead to the lower ratio of the successful manipulations, as shown in Fig. 1 (c). In order to improve the accuracy for positioning the tip, we put a nanoparticle around the nanotube. This nanoparticle can be used as a landmark which can be observed by local scanning in both the horizontal and the vertical directions. Then the tip position is estimated to improve the accuracy of positioning the tip around the nanotube. Finally, the results illustrate that the successful ratio is improved in the assembly task.

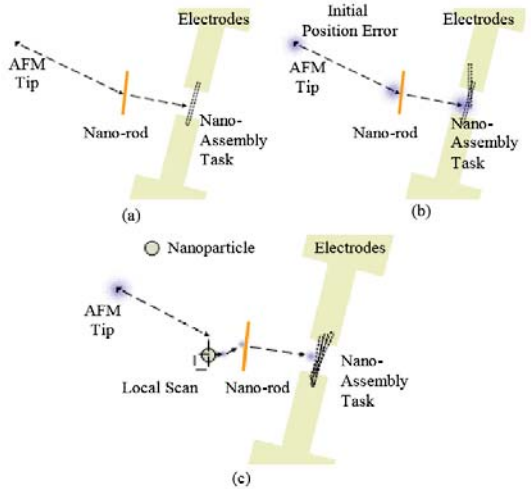

Fig. 1 Schematic diagram of device assembly based on AFM nano-manipulation

The tip position has uncertainty due to the influence of PZT nonlinearity and the system thermal drift [3,4]. The compensation methods of these two factors are analyzed and discussed as bellows.

There are two methods mainly used in the PZT

compensation model: one is the sensor-based closed-loop model, the other is the compensation method which is based on the open-loop model [5]. Closed-loop control model has a reliable compensation effect, so it is widely used nowadays. The compensation effect of this model depends heavily on the accuracy of the model parameters. However, the calibration process of the model parameters is time-consuming and is easily disturbed by the external factors.

As for the system thermal drift due to changes of ambient temperature and humidity, shrinkage and expansion rate of AFM mechanical parts are inconsistent, which results in the drift between the tip and the substrate sample [6,7,4]. To resolve this problem, the researchers introduce the SLAM method in the current macro-robot localization. The feature in the sample surface are regarded as the landmark [8], which is observed by the local scanning method in the task space. The tip position is estimated by observing the landmark, then the tip is moved to the target position for nanomanipulation [3]. After the landmark position is obtained, the tip position is estimated based on the relative distance between the tip and the landmark. The closer the tip position is to the landmark, the higher the accuracy of the tip position is. When the distance between the tip and the landmark is relatively far, after the tip moves to the target location, the accuracy of the positioning may not meet the requirements. So we need to push the landmark approaching the target location for active landmark configuration, which improves the accuracy of the tip positioning. As for a single sign in the task space, this paper presents a method of landmark based the probability distribution region to estimate the position of the tip.

Considering that the initial positions of the tip are different related to the landmark position, the simulation results illustrate that the tip positioning accuracy can be guaranteed after each observation of the landmark. As for the complicated situation of multiple landmarks in the task space, this paper proposes a path planning based on the probability distribution region. On the basis of the research work before, we define the observation distance between the adjacent landmarks and establish the landmark adjacency matrix between the multiple landmarks. Then we develop the path planning between the landmarks by using the shortest path algorithm. During the active landmark configuration, the landmark domain is proposed to provide a guidance for building the landmark. Finally, we construct a polygon with 15 nanoparticles and verify the effectiveness of the proposed method. The results show that it can help to improve the AFM nano-manipulation efficiency for Micro/Nano device assembly.

2. Accuracy Analysis of positioning tip using the landmark observation

2.1 Positioning AFM tip using landmark observation

The AFM tip position in the task frame is disturbed by system thermal drift and PZT nonlinearity. In the AFM tip task space, referring to the macroscopic robot positioning method, the position of the tip can be estimated according to the relative distance between the tip and the landmarks. In the task space, we find some features, such as nanoparticles. These features in the environment can maintain the same position and the feature can be used as a landmark. In the task space, we can look for some feature. These feature remain their position in uncertain environment, so they can be used as landmarks. The feature in the task space is selected for observation to localizing the tip referring to SLAM (Simultaneous Localization and Mapping) algorithm [9-11] which localizes the robot through measuring the distance from corner, plane, cylinder, and so on in Fig.2 (a). The example is described according to Fig.2 (b). The tip drifts in the task frame, and the nanoparticle P_0' is observed by the local scan including horizontal and vertical scan shown in Fig. 2(b) and Fig2. (c).

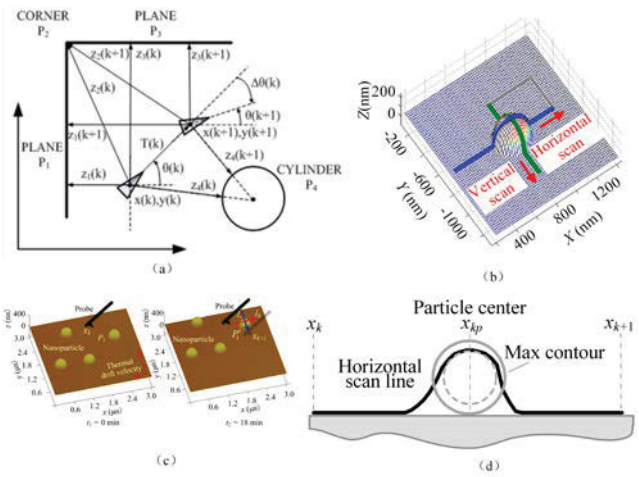

Fig. 2: Tip positioning strategy based on probability distribution interval

Fig. 2 (d) show that the horizontal observation similar to the vertical observation is modeled by following expressions:

2.1.1 Tip movement model

The tip movement model introduces the space state of the tip when the tip is moving.

$$x_{k+1} = g(x_k, u_k) + w_{k+1} \qquad w_{k+1} \sim N(0, R_{k+1}) \quad (1)$$

$$x_{kp} = x_k + l_{k1}^* \frac{x_{k,k+1}}{\| x_{k,k+1}^* \|} + w_{kp} \qquad w_{kp} \sim N(0, R_{kp}) \quad (2)$$

where x_{k+1} and x_k represent the positional state of the tip at k+1 or k. And $g(x_k, u_k)$ is the state transition function of the model[12-15]. w_{k+1} is a perturbation variable that satisfies the Gaussian distribution $N(0, R_{kp})$. w_{kp} is the perturbed random variable. l_{k1} represents a random variable from x_k to x_{k+1} in the scan path. l_{k1}^* is the mean of l_{k1}.

2.1.2 Landmark observation model

The observation model is the observation of the tip's position at x_{kp}, that is, at the time of k+1.

$$\hat{z}(kp) = h(\hat{x}(kp \mid k), m_j) + v_{z,kp} \qquad v_{z,kp} \sim N(0, Q_{z,kp}) \quad (3)$$

By using Kalman filtering to estimate, the observations can be inferred from the state values:

$$h(\hat{x}(kp \mid k), m_j) = x(kp \mid k) \quad (4)$$

$$h'(x_{kp}, m_j) = R_\theta^T (S_x R_\theta m_{j,xy} + S_x R_\theta x_{kp}) \quad (5)$$

Equation (5) is the rotation matrix of the local scanning direction. S_x and S_y are selection matrices.

$$S_x = \begin{pmatrix} 1 & 0 \\ 0 & 0 \end{pmatrix}, \quad S_y = \begin{pmatrix} 0 & 0 \\ 0 & 1 \end{pmatrix} \quad (6)$$

According to the observation model, it can be seen that a local scanning observation can only provide the updating of the tip position in one direction.

The tip positioning process includes the updating of the tip in the lateral direction of the task space coordinate system (horizontal and vertical directions).

2.2 Accuracy analysis of positioning tip using landmark observation

In the local scanning process, the nanoparticles need to be scanned in both horizontal and vertical direction. Then we positioned the four optional positions around the nanoparticles, as shown in Fig. 3.

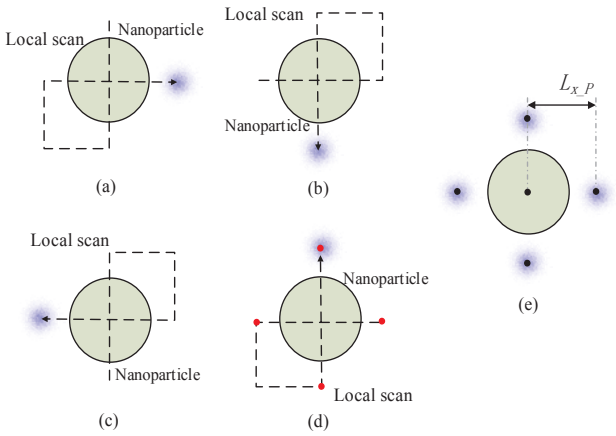

Fig. 3: Tip positioning near the nanoparticles

In order to achieve precise positioning of the tip, the initial conditions in a given nanomanipulation environment are:

- The initial error distribution of the tip.
- The coordinate position of the landmark in the task space.
- The location where the tip needs to operate.

2.2.1 Accuracy analysis of Tip Position in Different Initial Position

Aiming at the different position of the tip relative to the initial position of the nanoparticles, it is verified that the accuracy of the tip positioning after the landmark observation is consistent. In Fig. 4, the red dashed box shows the distribution range of the tip in the current position. The blue dashed box indicates the distribution range of the tip at the last time. By comparing the two results, it shows the change of the distribution range after moving. The red solid line indicates the path of the tip's local scan. Fig. 4(a) shows that the tip is moved from the initial position to the left side of the nanoparticles in a certain initial position distribution, and then the nanoparticles are scanned locally, and finally the position distribution is estimated below the nanoparticles. Fig. 4(b) shows the simulation results when the initial position distribution of the tip is increasing. Fig. 4(c) shows the results of the position estimation by local scanning in the case where the initial position of the tip is far from the nanoparticle.

Table 1 records the deviation in the two positions (Horizontal, vertical) at initial position, P_1, P_2, P_3, P_4, P_5. As shown in Fig. 4(a) - (c), the deviation at P_5 is close to 5nm. The positioning accuracy of the tip in the initial position is kept within a certain range, so the experimental results are consistent.

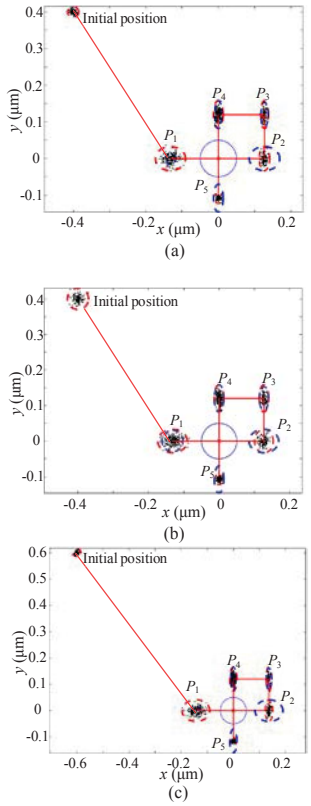

Fig. 4: Results of tip positioning under different initial conditions

Table 1: Standard deviation sigma of tip distribution at each location in Fig. 4 (Unit:*nm*)

	(a)	(b)	(c)
Initial	(5.0,5.0)	(10.0,10.0)	(5.0,5.0)
P_1	(14.0,11.0)	(14.0,11.0)	(17.8 13.7)
P_2	(3.5,11.0)	(4.4,11.0)	(3.5,13.7)
P_3	(3.5,12.7)	(4.4,12.7)	(3.5,15.1)
P_4	(4.4,12.7)	(4.5,12.7)	(4.5,15.1)
P_5	(4.4,4.8)	(4.5,4.8)	(4.5,4.8)

2.2.2 Accuracy analysis of tip position in different path

Based on the analysis of the positioning accuracy under the initial position of the tip, the consistency of the positioning accuracy of the four optional positions around the tip is further verified. The simulation experiment is as follows. Assuming that the initial position distribution of the tip is the same, we calculate the distribution deviation of the tip in four different positions, as shown in Fig. 5.

In Fig. 5, the red dashed box shows the distribution range of the tip in the current position. The blue dashed box indicates the distribution range of the tip at the last time. By comparing the two results, it shows the change of the distribution range after moving. The red solid line indicates the path of the tip's local scan. Fig. 5(a) - (d) show the simulation results for estimating the left, right, upper and lower positions of the nanoparticles. Table 2 records the deviation in the two positions (horizontal and vertical directions) at initial position, P_1, P_2, P_3, P_4, P_5 in the four positioning cases.

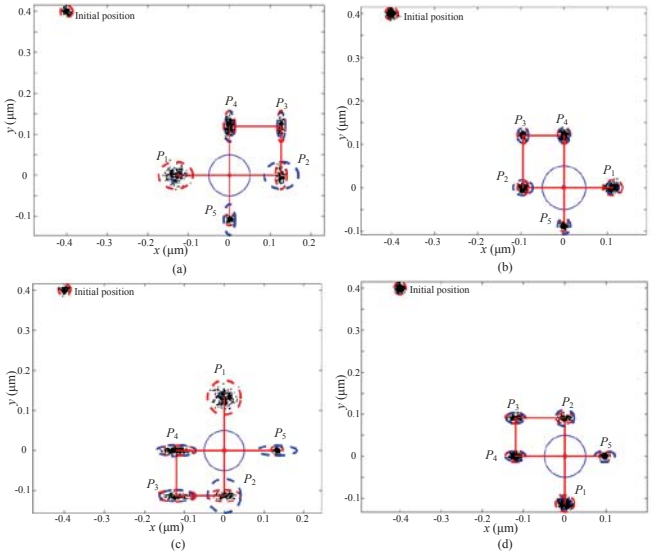

Fig. 5: the tip positioning process of four optional positions

Table 2: The error distribution of the tip in four different scan path in Fig. 5(Unit:*nm*)

	(a)	(b)	(c)	(d)
Initial	(5.0,5.0)	(5.0,5.0)	(5.0,5.0)	(5.0,5.0)
P_1	(14.0,11.0)	(7.6,5.9)	(14.0,14.2)	(7.6,6.5)
P_2	(13.5,11.0)	(4.3,5.9)	(14.0,4.8)	(7.6,4.2)
P_3	(13.5,12.7)	(4.3,6.2)	(6.5,4.8)	(8.1,8.1)
P_4	(4.4,12.7)	(5.0,6.2)	(6.5,4.2)	(8.1,4.5)
P_5	(4.4,4.8)	(5.0,4.0)	(4.9,4.2)	(4.4,4.5)

According to the data in Table 2, it can be seen that the change of the local scanning path of the tip has little effect on the positioning accuracy at the P_5 position, and the tip position distribution can guarantee the consistency.

3. A Method of Planning a Tip Path Based on the Probability Distribution Region

3.1 Observation distance between two landmarks

For only one landmark in the environment, we can use local scan method [12-14]. And we can know the is:

$$P_{j\_0} * L_{j\_0} + \sum_{k=1}^{n-1} P_{j\_k} * (L_{j\_k} + u_{y\_k+1}) \tag{7}$$

For multi-landmark environment, the tip needs to select the relevant observation landmarks for path planning. Here we use the observation distance between two landmarks as the weight to establish the adjacency matrix of multiple landmarks. The shortest path algorithm and ant colony algorithm are used for landmark selection and path planning.

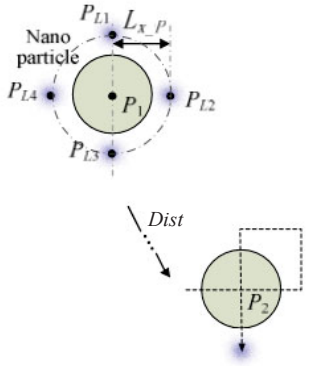

Fig. 6: The shortest observation distance between landmarks

On the basis of (7), the shortest observation distance of the tip from nanoparticle m_i to m_j is defined as $L_{p\_i,j}$:

$$L_{p\_i,j} = scantimes * (P_{j\_0} * (L_{j\_0} + Dist / D_r) + \sum_{k=1}^{n-1} P_{j\_k} * (L_{j\_k} + u_{y\_k+1})) \tag{8}$$

Where *Dist* is the movement distance of the tip from the locating point P_{L3} to the left side of the nanoparticle P_2. And *Dr* is the side length of the square space where the nanoparticles are located.

Equation (8) indicates that the observation distance formed during the process from positioning at the vicinity of the nanoparticle mi to observing nanoparticle m_j.

Definition 1: The landmark sets $M = [m_1, m_2, ..., m_n]$, where $m_1 = (x_1, y_1)$, x_i, y_i is the coordinates of the landmark m_i in the task space, $i = 1, 2, ..., n$.

Definition 2: the adjacency matrix of landmarks

$$W = \begin{bmatrix} 0 & w_{12} & w_{13} & w_{14} & \cdots & w_{1n} \\ w_{21} & 0 & w_{23} & w_{24} & \cdots & w_{2n} \\ w_{31} & w_{32} & 0 & w_{34} & \cdots & w_{3n} \\ w_{41} & w_{42} & w_{43} & 0 & \cdots & w_{4n} \\ \cdots & \cdots & \cdots & \cdots & \cdots & \cdots \\ w_{n1} & w_{n2} & w_{n3} & w_{n4} & \cdots & 0 \end{bmatrix} \tag{9}$$

The weight w_{ij} represents the observation distance of the landmark from m_i to m_j. If $i = j$, then $w_{ij} = 0$.

3.2 Path planning of the tip observing and manipulation

Fig. 7 shows that there are six landmarks(P_1、P_2、P_3、P_4、P_5、P_6) in the task space. Assuming that the tip is positioned as an initial position after positioning the P_1 nanoparticles, the tip needs to move to the vicinity of nanoparticle P_6 to perform nanometer operation. In order to ensure the shortest observation distance when the tip moves to the P_6, we use the Dijkstra algorithm for path planning. The data in Table 3 is the observation distance between each two landmarks which form the adjacency matrix.

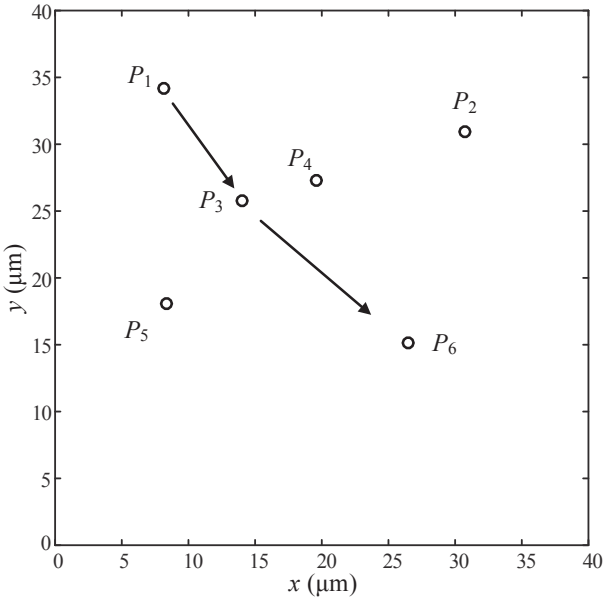

Fig. 7: Path planning based on Dijkstra algorithm

Table 3: Adjacency matrix of landmarks (Unit: μm)

	P_1	P_2	P_3	P_4	P_5	P_6
P_1	0.0000	0.7697	1.0054	0.9678	3.1106	3.1856
P_2	0.7697	0.0000	0.9222	0.7295	1.0197	3.1108
P_3	1.0054	0.9222	0.0000	0.6956	0.9858	1.0095
P_4	0.9678	0.7295	0.6956	0.0000	1.0065	3.0627
P_5	3.1106	1.0197	0.9858	1.0065	0.0000	0.7792
P_6	3.1856	3.1108	1.0095	3.0627	0.7792	0.0000

The simulation results show that P_1, P_3, P_6 can be observed by the tip through the local scan. At the same time, the tip can be quickly moved to the nanoparticle P_6 through the minimum "cost". If the target position is far away from the nanoparticle P_6, the positioning accuracy of the tip may not meet the precision when the tip is moved to the target position, then we need the active landmark configuration referring to the macroscopic robot positioning method.

4. Experimental Results

In this section, the effectiveness of the above-mentioned tip path planning method in nanomanipulation is experimentally verified.

In the task space, 16 nanoparticles are distributed. As shown in Fig. 8(a), it is necessary to control the tip to push the 15 nanoparticles into a pentadecagon and push the other to the specified position. The direction of the action of each nanoparticle is shown by the white arrow in Fig. 8(a), and finally the result shown in Fig. 8(b) is formed.

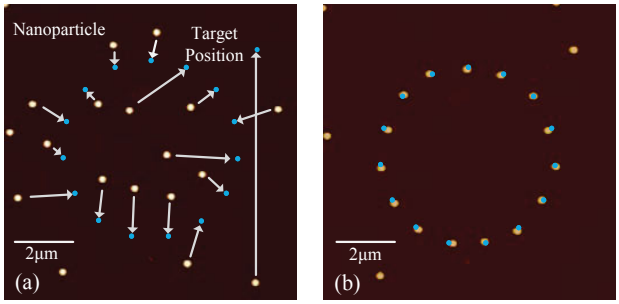

Fig. 8: Position distribution and configuration requirements of nanoparticles in the task space

During the operation of the nanoparticles, the initial positions of each nanoparticle and their corresponding target positions are first determined and each nanoparticle is numbered. And then push each nanoparticle in sequence. When a nanoparticle is pushed to the target position, the tip moves to the next nanoparticle for local scanning, and after the tip is positioned, the operation is continued until the operation is completed. We define the distance between the current target position and the next possible nanoparticle as observation distance to create an adjacency matrix, as shown in Table 4. Under the premise of ensuring the accuracy of the tip positioning, we select the optimal path of the tip observation path and operation path. The blue circle in Fig. 9 represents the initial position of each nanoparticle and the black circle represents the target position. The dashed arrow between the target position and the initial position is the optimal planning path obtained by using the ant colony optimization algorithm. Thus, the nanoparticles are operated in the order of 15, 12, 13, 14, 16, 1, 11, 10, 2, 7, 8, 3, 4, 6, 5, 9, and the tip push the nanoparticles to the target position, finally establishing the nanoparticle structure.

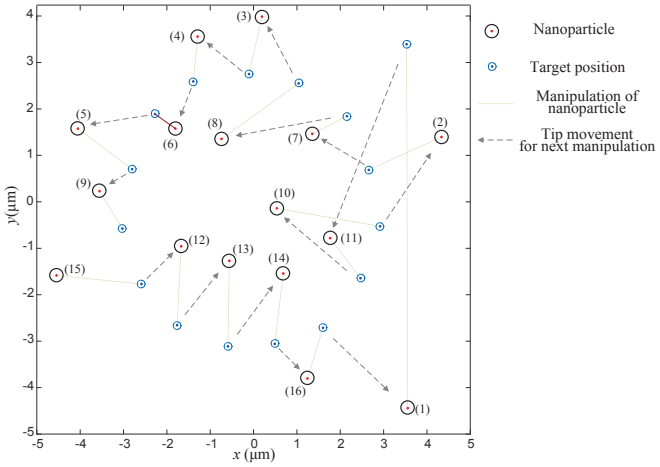

Fig. 9: Path planning based on ant colony optimization

Table 4: Adjacent matrices of nanoparticles in the task space (Unit: μm)

	P_1	P_2	P_3	P_4	P_5	P_6	P_7	P_8	P_9	P_{10}	P_{11}	P_{12}	P_{13}	P_{14}	P_{15}	P_{16}
P_1	0.0000	0.4024	0.6482	0.6801	0.5847	0.6563	0.5082	0.5965	0.5006	0.3049	0.2360	0.3139	0.2458	0.2124	0.4013	0.1947
P_2	0.4024	0.0000	0.2571	0.2911	0.3012	0.2703	0.1388	0.2079	0.4015	0.1900	0.2714	0.4933	0.4779	0.4331	0.4661	0.3704
P_3	0.6482	0.2571	0.0000	0.1659	0.3221	0.2316	0.2184	0.1485	0.4194	0.4000	0.4743	0.5517	0.5679	0.5545	0.4987	0.5444
P_4	0.6801	0.2911	0.1659	0.0000	0.2498	0.1645	0.2431	0.1695	0.3442	0.4201	0.4861	0.4847	0.5283	0.5452	0.4263	0.5447
P_5	0.5847	0.3012	0.3221	0.2498	0.0000	0.1214	0.2418	0.2564	0.1939	0.3958	0.4532	0.3660	0.4368	0.4720	0.2814	0.4916
P_6	0.6563	0.2703	0.2316	0.1645	0.1214	0.0000	0.1799	0.1840	0.1987	0.3114	0.3638	0.3190	0.3742	0.3963	0.2671	0.4056
P_7	0.5082	0.1388	0.2184	0.2431	0.2418	0.1799	0.0000	0.1187	0.2950	0.1981	0.2573	0.3837	0.3826	0.3546	0.3523	0.3181
P_8	0.5965	0.2079	0.1485	0.1695	0.2564	0.1840	0.1187	0.0000	0.2163	0.2600	0.3109	0.3191	0.3384	0.3533	0.2763	0.3557
P_9	0.5006	0.4015	0.4194	0.3442	0.1939	0.1987	0.2950	0.2163	0.0000	0.2858	0.3451	0.2592	0.3250	0.3597	0.1835	0.3801
P_{10}	0.3049	0.1900	0.4000	0.4201	0.3958	0.3114	0.1981	0.2600	0.2858	0.0000	0.1819	0.2509	0.2485	0.2262	0.2274	0.2210
P_{11}	0.2360	0.2714	0.4743	0.4861	0.4532	0.3638	0.2573	0.3109	0.3451	0.1819	0.0000	0.2549	0.2415	0.2075	0.2332	0.1649
P_{12}	0.3139	0.4933	0.5517	0.4847	0.3660	0.3190	0.3837	0.3191	0.2592	0.2509	0.2549	0.0000	0.1953	0.2218	0.1182	0.2394
P_{13}	0.2458	0.4779	0.5679	0.5283	0.4368	0.3742	0.3826	0.3384	0.3250	0.2485	0.2415	0.1953	0.0000	0.1729	0.1366	0.1859
P_{14}	0.2124	0.4331	0.5545	0.5452	0.4720	0.3963	0.3546	0.3533	0.3597	0.2262	0.2075	0.2218	0.1729	0.0000	0.1589	0.1359
P_{15}	0.4013	0.4661	0.4987	0.4263	0.2814	0.2671	0.3523	0.2763	0.1835	0.2274	0.2332	0.1182	0.1366	0.1589	0.0000	0.3007
P_{16}	0.1947	0.3704	0.5444	0.5447	0.4916	0.4056	0.3181	0.3557	0.3801	0.2210	0.1649	0.2394	0.1859	0.1359	0.3007	0.0000

5. Conclusion

In this paper, for improving the low efficiency of nanomanipulation caused by the uncertainty of the tip position in AFM nano-manipulation, we propose the path planning and design a method of nanometer manipulating robot based on the probability distribution interval after establishing the driving model and landmark observation model. Based on the local path analysis of the tip, the adjacent matrix is constructed using the observation distance, and the operation path of the AFM tip is planned by using the shortest path algorithm and the ant colony algorithm. The simulation results show that the AFM tip path planning method can optimize the tip path in the multi-paths environment, and improve the efficiency of the nano-manipulation and promote the practical application of AFM nano-manipulation for the assembly of the nano-manipulation devices.

References

[1] L. Hans, "Semiconductor nanostructures: a new impact on electronics," Applied Surface Science, vol. 130-132, pp. 855-865, 1998.

[2] B. Bhushan, Springer Handbook of Nano-technology, Springer press, New York, 2005.

[3] Yuan S., Liu L.Q., and et al.. "Feature referenced tip localization enhanced by probability motion model for AFM based nanomanipulations". IEEE ROBIO 2011, Phuket Thailand. pp. 1421-1426, 2011.

[4] Liu L.Q., Luo Y.L., and et al.. "Sensor Referenced Real-Time Videolization of Atomic Force Microscopy for Nanomanipulations,"Mechatronics,IEEE/ASME Transactions on, Volume. 13, no. 1, pp. 76-85, 2008.

[5] G.Y. Li, et al., "Development of augmented reality system for AFM-based nanomanipulation" IEEE-ASME T. Mech., vol. 9, no. 2, pp. 358-365, 2004.

[6] Krohs F., Onal C., and et al. "Towards Automated Nanoassembly with the Atomic Force Microscope: A Versatile Drift Compensation Procedure," Journal of Dynamic Systems, Measurement, and Control, Volume. 131, no. 3, pp. 061106,2009.

[7] Wang Z.Y., Liu L.Q., and et al. "AFM Tip On-Line Positioning by Using the Landmark" IEEE ROBIO 2011, Phuket Thailand. pp. 923-928,2011.

[8] L.Q. Liu, et al., "Sensor Referenced Real-Time Videolization of Atomic Force Microscopy for Nanomanipulations" IEEE-ASME T. Mech.., vol. 13, no. 1, pp. 76-85, 2008.

[9] S.Thrun,et al.,Probabilistic Robotics. London,England:The MIT Press, Cambridge, Massachusetts, 2005.

[10] J. J. Leonard and H. F. Durrant-Whyte, "Mobile robot localization by tracking geometric beacons" IEEE T. Robot. Atom., vol. 7, no. 3, pp. 376-382, 1991.

[11] Thrun S.. "Probabilistic Robotics," Commun. ACM, Volume. 45, pp. 52-57, 2002.

[12] S.Yuan, et al., "A probabilistic approach for on-line positioning in nano manipulations". IEEE WCICA 8th, JiNan, pp. 450, 2010.

[13] S.Yuan, et al., "AFM Tip On-Line Positioning by Using the Landmark". IEEE NMDC 10th , CA, pp. 75, 2010.

[14] K. Kuhnen and H.Janocha, "Inverse feedforward controller for complex hysteretic nonlinearities in smart-material systems" Control Intell.Syst.,vol. 29, no. 3, pp. 74–83, 2001.

[15] S.Yuan, Z.D.,Wang, L.Q. Liu, N. Xi, Y.C. Wang, "Stochastic Approach for Feature-based Localization and Planning in Nano-manipulations",IEEE Transactions on Automation Science and Engineering, 14(4): 1643-1654 ,2017